Measuring Polarization Dependant Frequency in DPSK Demodulators

Jean-Joseph Max [a], Sylvain O'Reilly [b]
[a]Avensys Inc., 400 Montpellier Blvd, Montreal, QC, Can,
[b]ITF Labs, 400 Montpellier Blvd, Montreal, QC, Can

ABSTRACT

We present a robust post-processing technique to extract the polarization dependant frequency (PDF) and Polarization dependant loss (PDL) from stokes measurements of differential phase shift keying (DPSK) demodulators. The present method is based on sine-fitting on transmissions. It evaluates PDF and PDL from sinus parameters (phase, amplitude and amplitude offset) through a Müller matrix analysis.

Keywords: DPSK, Polarization dependant frequency, PDL, Müller analysis.

1. INTRODUCTION

The Differential Phase Shift Keying (DPSK) demodulator is based on a Mach-Zehnder (MZ) interferometer. That interferometer consists of splitting light in two branches, delaying a branch and recombining. The optical phase retardation between branches of a MZ interferometer being proportional to the frequency of the optical wave, the transmission spectrum exhibits a sinusoidal response.

However, the MZ response can be different depending on the polarization of the incoming light. Although this impacts several parameters, more interest is put on the Polarization Dependant Frequency (PDF) and in a lesser extent, the Polarization Dependant Losses (PDL). The PDF measurement is hard to obtain directly or is obtained trough a yet unclear post-processing of the Stokes measurements. The purpose of this document is to clarify how PDF can be efficiently retrieved from Stokes measurements.

In the following document, DPSK demodulators will be modeled as a sinus with few parameters to measure and to fit. The Stokes measurements and Müller analysis will then be presented in a context of a MZ interferometer. A post-processing scheme is derived from these measurements as an extension of a widely spread PDL post-processing technique.

2. MODELING OF A DPSK TRANSMISSION

DPSK demodulators are delay line interferometers (DLI). An example of transmission spectrum of DPSK 66.7 GHz is shown in Figure 1 over the 1460–1580 nm range.

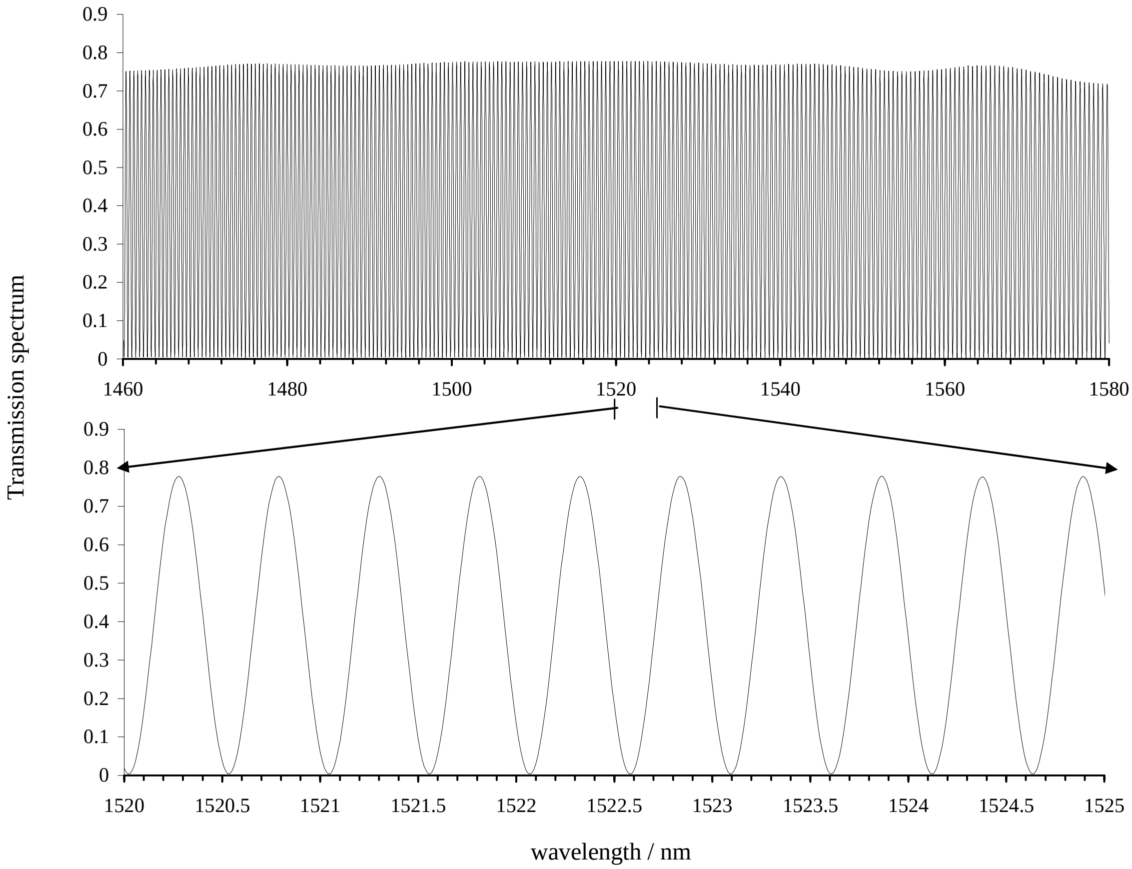

Figure 1 : Experimental transmission spectrum for a given polarization

Fitting the transmission using a single sine wave leads to very low residues (experimental minus fitted spectra). Transmissions T_i over the 1460–1580 nm range have been fitted using the simple expression:

$$T_i(\nu) = \frac{\eta_i}{2} \times \left[1 + \sin\left(2\pi \frac{\nu}{FSR} - \varphi_i \right) \right] + \varepsilon_i \qquad (2.1.1)$$

ν is the optical frequency, *FSR* is the free spectral range (the period of the interferometer), η_i is the amplitude of the modulation, φ_i is the phase at null frequency, and ε_i is a small offset, the lowest transmission level of the interferometer related to input polarization *i*.

It is observed in Figure 1 that the transmission maximum is not constant throughout the entire wavelength range. This exemplifies the slow variation of the sine wave produced by the device with the wavelength, namely: amplitude (A_i), phase (φ_i) and offset (ε_i) slowly vary with wavelength. Taking into account the slow variations of the parameters in eq. 2.1.1 with wavelength, discrepancies between sine fitting and experimental data can be reduced by more than a factor of 10.

From this we conclude that:

- DLI outputs are true sine functions of frequency;
- The *FSR* is almost independent of the input polarization (and of the output port)
- The DPSK transmission can be represented by a complex number of amplitude η_i and phase φ_i: $\eta_j \times e^{j\varphi_i}$;

Variation of φ_i with the polarization is due to *PDF* and variation of η_i and ε_i are due to *PDL*. Both are evaluated using Stokes-Müller method.

3. PDF AND PDL

This section will cover all the analysis leading to PDF post-processing. Starting with definition of Stokes measurements in DPSK demodulator, the $m_{1,j}$ are then evaluated. A discussion follows on the meaning of these elements. The PDF and PDL calculations are presented at the end of the section.

3.1 Stokes vector and Müller matrix

The Stokes vector S = *(S0, S1, S2, S3)* completely describes the power and polarization state of an optical wave (ref. 2). Each element of the vector is based on measured power levels. *S0* is the total intensity. *S1* describes the amount of linear horizontal (*S1*>0) or vertical polarization (*S1*<0). *S2* describes the amount of linear +45° (*S2*>0) or -45° (*S2*<0) polarization, and *S3* describes the amount of right-hand (*S3*>0) or left-hand circular (*S3*<0) polarization (refs. 1, 2). Using the Müller matrix, the output vector of a device under test is given by:

$$S0_{out} = m_{11}S0_{in} + m_{12}S1_{in} + m_{13}S2_{in} + m_{14}S3_{in} \qquad (3.1.1)$$

Where the $m_{1,j}$ are the first row elements of the Müller matrix. The first step is dedicated to get the characteristics of the transmission for each of the four different input vectors.

The four polarizations that build up the Stokes input vector are given in Table 1. The phases at null frequency of the respective transmitted signals are evaluated using a sine fitting procedure following equation 2.1.1. The parameters obtained are defined in following equation:

$$\begin{cases} T_a = \dfrac{\eta_1}{2}\left[1+\sin\left(\dfrac{2\pi\nu}{FSR}+\varphi_1\right)\right]+\varepsilon_1 = m_{11}+m_{12} \\ T_b = \dfrac{\eta_2}{2}\left[1+\sin\left(\dfrac{2\pi\nu}{FSR}+\varphi_2\right)\right]+\varepsilon_2 = m_{11}-m_{12} \\ T_c = \dfrac{\eta_3}{2}\left[1+\sin\left(\dfrac{2\pi\nu}{FSR}+\varphi_3\right)\right]+\varepsilon_3 = m_{11}+m_{13} \\ T_d = \dfrac{\eta_4}{2}\left[1+\sin\left(\dfrac{2\pi\nu}{FSR}+\varphi_4\right)\right]+\varepsilon_4 = m_{11}+m_{14} \end{cases} \qquad (3.1.2)$$

Table 1: Phase shift and polarization states input.

	Polarization description	Phase and amplitude of the transmission	Phase shift vs $\varphi_{11} = \dfrac{\varphi_1+\varphi_2}{2}$
P_a	$\begin{pmatrix}1\\1\\0\\0\end{pmatrix}$	$\begin{cases}\varphi_1 = \varphi_{11} + \dfrac{\varphi_1-\varphi_2}{2} \\ \eta_1\end{cases}$	$\dfrac{\varphi_1-\varphi_2}{2}$

	Polarization description	Phase and amplitude of the transmission	Phase shift vs $\varphi_{11} = \dfrac{\varphi_1 + \varphi_2}{2}$
P_b	$\begin{pmatrix} 1 \\ -1 \\ 0 \\ 0 \end{pmatrix}$	$\begin{cases} \varphi_2 = \varphi_{11} - \dfrac{\varphi_1 - \varphi_2}{2} \\ \eta_2 \end{cases}$	$-\dfrac{\varphi_1 - \varphi_2}{2}$
P_c	$\begin{pmatrix} 1 \\ 0 \\ 1 \\ 0 \end{pmatrix}$	$\begin{cases} \varphi_3 = \varphi_{11} + \left(\varphi_3 - \dfrac{\varphi_1 - \varphi_2}{2} \right) \\ \eta_3 \end{cases}$	$\varphi_3 - \dfrac{\varphi_1 + \varphi_2}{2}$
P_d	$\begin{pmatrix} 1 \\ 0 \\ 0 \\ 1 \end{pmatrix}$	$\begin{cases} \varphi_4 = \varphi_{11} + \left(\varphi_4 - \dfrac{\varphi_1 - \varphi_2}{2} \right) \\ \eta_4 \end{cases}$	$\varphi_4 - \dfrac{\varphi_1 + \varphi_2}{2}$

3.2 Evaluation of the $m_{1,j}$ elements

From eq. 3.1.2 one easily gets:

$$\begin{aligned} m_{11} = {} & \frac{\eta_1 + \eta_2}{4}\left[1 + \sin\left(\frac{2\pi\nu}{FSR} + \frac{\varphi_1 + \varphi_2}{2}\right)\cos\left(\frac{\varphi_1 - \varphi_2}{2}\right)\right] \\ & + \frac{\eta_1 - \eta_2}{4}\sin\left(\frac{\varphi_1 - \varphi_2}{2}\right)\cos\left(\frac{2\pi\nu}{FSR} + \frac{\varphi_1 + \varphi_2}{2}\right) + \frac{\varepsilon_1 + \varepsilon_2}{2} \end{aligned} \tag{3.2.1}$$

And

$$\begin{aligned} m_{12} = {} & \frac{\eta_1 + \eta_2}{4}\sin\left(\frac{\varphi_1 - \varphi_2}{2}\right)\cos\left(\frac{2\pi\nu}{FSR} + \frac{\varphi_1 + \varphi_2}{2}\right) \\ & + \frac{\eta_1 - \eta_2}{4}\cos\left(\frac{\varphi_1 - \varphi_2}{2}\right)\sin\left(\frac{2\pi\nu}{FSR} + \frac{\varphi_1 + \varphi_2}{2}\right) + \frac{\varepsilon_1 - \varepsilon_2}{2} \end{aligned} \tag{3.2.2}$$

Further, from eq. 3.1.2, the third element of the Muller 1st row can be written as follows:

$$m_{13}=\begin{cases}\alpha\cos\left(\dfrac{\varphi_1-\varphi_2}{2}\right)\sin(\chi)\cos\left(\dfrac{2\pi\nu}{FSR}+\psi\right)\\+\gamma\left[1+\cos\left(\dfrac{\varphi_1-\varphi_2}{2}\right)\sin\left(\dfrac{2\pi\nu}{FSR}+\psi\right)\cos(\chi)\right]\\+\dfrac{\eta_3}{2}\left[1-\cos\left(\dfrac{\varphi_1-\varphi_2}{2}\right)\right]\sin\left(\dfrac{2\pi\nu}{FSR}+\varphi_3\right)\\-\dfrac{\eta_1-\eta_2}{4}\sin\left(\dfrac{\varphi_1-\varphi_2}{2}\right)\cos\left(\dfrac{2\pi\nu}{FSR}+\dfrac{\varphi_1+\varphi_2}{2}\right)+\varepsilon_3-\dfrac{\varepsilon_1+\varepsilon_2}{2}\end{cases}\qquad(3.2.3)$$

Where:

$$\psi=\frac{\varphi_3+\dfrac{\varphi_1+\varphi_2}{2}}{2}$$

$$\chi=\frac{\varphi_3-\dfrac{\varphi_1+\varphi_2}{2}}{2}$$

$$\alpha=\frac{\eta_3+\dfrac{\eta_1+\eta_2}{2}}{2}$$

$$\gamma=\frac{\eta_3-\dfrac{\eta_1+\eta_2}{2}}{2}$$

One can see that ψ is a 0^{th} order phase term and α is a 0^{th} order amplitude term, while χ and γ are of the 1^{st} order phase and amplitude respectively.

And finally the last element being :

$$m_{14}=\begin{cases}\beta\cos\left(\dfrac{\varphi_1-\varphi_2}{2}\right)\sin(\kappa)\cos\left(\dfrac{2\pi\nu}{FSR}+\rho\right)\\+\mu\left[1+\cos\left(\dfrac{\varphi_1-\varphi_2}{2}\right)\sin\left(\dfrac{2\pi\nu}{FSR}+\rho\right)\cos(\kappa)\right]\\+\dfrac{\eta_4}{2}\left[1-\cos\left(\dfrac{\varphi_1-\varphi_2}{2}\right)\right]\sin\left(\dfrac{2\pi\nu}{FSR}+\varphi_4\right)\\-\dfrac{\eta_1-\eta_2}{4}\sin\left(\dfrac{\varphi_1-\varphi_2}{2}\right)\cos\left(\dfrac{2\pi\nu}{FSR}+\dfrac{\varphi_1+\varphi_2}{2}\right)+\varepsilon_3-\dfrac{\varepsilon_1+\varepsilon_2}{2}\end{cases}\qquad(3.2.4)$$

where

$$\rho = \frac{\varphi_4 + \frac{\varphi_1 + \varphi_2}{2}}{2}$$

$$\kappa = \frac{\varphi_4 - \frac{\varphi_1 + \varphi_2}{2}}{2}$$

$$\beta = \frac{\eta_4 + \frac{\eta_1 + \eta_2}{2}}{2}$$

$$\mu = \frac{\eta_4 - \frac{\eta_1 + \eta_2}{2}}{2}$$

One can see that ρ and β are of the 0^{th} order in phase and amplitude respectively, while κ and μ are of the 1^{st} order in phase and amplitude respectively.

Signification of the terms of the $m_{1,j}$ elements

Looking at the $m_{1,j}$ elements, on can get physical insight of the PDL and PDF contributions trough the Müller analysis. Devices to be tested being low PDL and low PDF components, the following conditions are satisfied:

$$\begin{cases} \left|\eta_i - \eta_j\right| << 1 \\ \left|\varphi_i - \varphi_j\right| << \frac{\pi}{2} \end{cases} \tag{3.2.5}$$

Eq. 3.2.1 can be approximated by:

$$m_{11} \approx \begin{cases} \frac{\eta_1 + \eta_2}{4}\left[1 + \sin\left(\frac{2\pi\nu}{FSR} + \frac{\varphi_1 + \varphi_2}{2}\right) \times \left(1 - \frac{\left[\varphi_1 - \varphi_2\right]^2}{8}\right)\right] \\ + \frac{\eta_1 - \eta_2}{4} \times \frac{\varphi_1 - \varphi_2}{2}\cos\left(\frac{2\pi\nu}{FSR} + \frac{\varphi_1 + \varphi_2}{2}\right) \\ + \frac{\varepsilon_1 + \varepsilon_2}{2} \end{cases} \tag{3.2.6}$$

The 1^{st} term in eq. 3.2.6 is of 0^{th} order in amplitude. The second term is of 2^{nd} order (one order in the phase difference × one in the amplitude difference). It therefore can be neglected. Hence, m_{11} is a true sine wave.

From eq. 3.2.2 one gets:

$$m_{12} \approx \begin{cases} \dfrac{\eta_1+\eta_2}{4}\times\dfrac{\varphi_1-\varphi_2}{2}\cos\left(\dfrac{2\pi\nu}{FSR}+\dfrac{\varphi_1+\varphi_2}{2}\right) \\ +\dfrac{\eta_1-\eta_2}{4}\left[1-\dfrac{(\varphi_1-\varphi_2)^2}{8}\right]\sin\left(\dfrac{2\pi\nu}{FSR}+\dfrac{\varphi_1+\varphi_2}{2}\right) \\ +\dfrac{\varepsilon_1-\varepsilon_2}{2} \end{cases} \qquad (3.2.7)$$

The 1st term in eq. 3.2.7 is a 1st order one (1st order in the phase difference × 0th in the amplitude difference). This term is a cosine: it is $\pi/2$ shifted compared to m_{11}. It therefore is a *PDF* contributor (it will slightly modify the device phase at null frequency). The 2nd term in eq. 3.2.7 is a 1st order one (1st in the amplitude difference × 0th order in the phase difference). This term is a sine: it is in phase with m_{11}. It therefore is a *PDL* contributor (it will not affect the device phase at null frequency). Last term in eq. 3.2.7 is a negligible offset.

Approximation of eq. 3.2.3 can be written as follows:

$$m_{13} = \begin{cases} \alpha\chi\left[1-\dfrac{(\varphi_1-\varphi_2)^2}{8}\right]\cos\left(\dfrac{2\pi\nu}{FSR}+\psi\right) \\ +\gamma\left[1+\left\{1-\dfrac{(\varphi_1-\varphi_2)^2+\chi^2}{8}\right\}\sin\left(\dfrac{2\pi\nu}{FSR}+\psi\right)\right] \\ +\dfrac{\eta_3}{2}\times\dfrac{(\varphi_1-\varphi_2)^2}{8}\sin\left(\dfrac{2\pi\nu}{FSR}+\varphi_3\right) \\ -\dfrac{\eta_1-\eta_2}{4}\times\dfrac{\varphi_1-\varphi_2}{2}\cos\left(\dfrac{2\pi\nu}{FSR}+\dfrac{\varphi_1+\varphi_2}{2}\right)+\varepsilon_3-\dfrac{\varepsilon_1+\varepsilon_2}{2} \end{cases} \qquad (3.2.8)$$

The 1st term in eq. 3.2.8 is of 1st order. This term is a cosine: it is ~$\pi/2$ shifted compared to m_{11}. It therefore is a *PDF* contributor.

The 2nd term in eq. 3.2.8 is also of the 1st order. This term is a sine: it is nearly in phase with m_{11}. It therefore is a *PDL* contributor. This term also contributes to the offset of m_{13}.

The two next terms are 2nd order ones. These can therefore be neglected. Last term in eq. 3.2.8 is a negligible offset.

Finally, an approximation of eq. 3.2.4 is given by:

$$m_{14} = \begin{cases} \beta\kappa\left\{1 - \frac{(\varphi_1 - \varphi_2)^2}{8}\right\}\cos\left(\frac{2\pi\nu}{FSR} + \rho\right) \\ + \mu\left[1 + \left\{1 - \frac{(\varphi_1 - \varphi_2)^2 + \kappa^2}{8}\right\}\sin\left(\frac{2\pi\nu}{FSR} + \rho\right)\right] \\ + \frac{\eta_4}{2} \times \frac{(\varphi_1 - \varphi_2)^2}{8}\sin\left(\frac{2\pi\nu}{FSR} + \varphi_4\right) \\ - \frac{\eta_1 - \eta_2}{4} \times \frac{\varphi_1 - \varphi_2}{2}\cos\left(\frac{2\pi\nu}{FSR} + \frac{\varphi_1 + \varphi_2}{2}\right) \\ + \varepsilon_4 - \frac{\varepsilon_1 + \varepsilon_2}{2} \end{cases} \tag{3.2.9}$$

Similarly to m_{13}, the 1^{st} term in eq. 3.2.9 is of the 1^{st} order. This term is a cosine: it is ~π/2 shifted compared to m_{11}. It therefore is a *PDF* contributor.

The 2^{nd} term in eq. 3.2.9 is of the 1^{st} order. This term is a sine: it is nearly in phase with m_{11}. It therefore is a *PDL* contributor. This term also contributes to the offset of m_{14}.

The two next terms are 2^{nd} order one. These can therefore be neglected. Last term in eq. 3.2.9 is a negligible offset.

Above discussion permits to separate the elements that contribute to the device *PDF* from those that contribute to its *PDL*.

3.3 Evaluation of the extreme transmission along the Poincaré sphere

According to the Stokes vector polarization description and the Müller transfer matrix, the device transmission under totally polarized input power is given by (ref. 1):

$$\begin{cases} T = m_{11} + m_{12}x_1 + m_{13}x_2 + m_{14}x_3 \\ x_1^2 + x_2^2 + x_3^2 = 1 \end{cases} \tag{3.3.1}$$

in which x_i are the polarization components on the Poincaré sphere.

We are looking at the phase and amplitude of the comb that the transmission spectrum produces. Considering the terms of the m_{1j} (j = 2, 3, 4) that are shifted from that of m_{11} by ± π/2 (see eq. 3.2.6 to 3.2.9) and since their respective amplitudes η_{1j} are one order of magnitude lower than that of m_{11}, the phase shift (from the m_{11} phase) can simply be evaluated by the following approximation:

$$\eta_{11}\tan(\Delta\varphi) = x_1\eta_{12} + x_2\eta_{13} + x_3\eta_{14} \tag{3.3.2}$$

The problem is now to look for maximum and minimum of Δφ that will represent the maximum phase shift under the input polarization possible variation. This problem is simply dealt with using Lagrange multipliers. We built the function:

$$H = x_1\eta_{12} + x_2\eta_{13} + x_3\eta_{14} + \lambda\left(x_1^2 + x_2^2 + x_3^2 - 1\right) \tag{3.3.3}$$

Looking for the sets of value that give a null derivative for H is equivalent to our initial problem because $x_1^2 + x_2^2 + x_3^2 - 1$ is a constant. Hence,

$$\begin{cases} \dfrac{\partial H}{\partial x_1} = \eta_{12} + 2\lambda x_1 = 0 \\ \dfrac{\partial H}{\partial x_2} = \eta_{13} + 2\lambda x_2 = 0 \\ \dfrac{\partial H}{\partial x_3} = \eta_{14} + 2\lambda x_3 = 0 \end{cases} \tag{3.3.4}$$

That solves into

$$\begin{cases} x_1 = -\dfrac{\eta_{12}}{2\lambda} \\ x_2 = -\dfrac{\eta_{13}}{2\lambda} \\ x_3 = -\dfrac{\eta_{14}}{2\lambda} \end{cases} \tag{3.3.5}$$

From eq. 3.3.5 and the condition $x_1^2 + x_2^2 + x_3^2 = 1$ we get:

$$2\lambda = \sqrt{\eta_{12}^2 + \eta_{13}^2 + \eta_{14}^2} \tag{3.3.6}$$

Finally:

$$\tan(\Delta\varphi_{\max}) = \pm \frac{\sqrt{\eta_{12}^2 + \eta_{13}^2 + \eta_{14}^2}}{\eta_{11}} \tag{3.3.7}$$

Finally, we get the PDF value corresponding to the maximum span of the transmission phase at null frequency:

$$PDF = 2\frac{\Delta\varphi_{\max}}{2\pi} \times FSR \approx \frac{\sqrt{\eta_{12}^2 + \eta_{13}^2 + \eta_{14}^2}}{\pi \times \eta_{11}} \times FSR \tag{3.3.8}$$

Replacing the η_{1j} in eq. 3.3.8 by their values from eq. 3.2.7 to 3.2.9 (the amplitudes of the cosine terms at the 1st order) one gets:

$$PDF \approx \frac{\sqrt{\left(\dfrac{\varphi_1 - \varphi_2}{2}\right)^2 + \left(\varphi_3 - \dfrac{\varphi_1 + \varphi_2}{2}\right)^2 + \left(\varphi_4 - \dfrac{\varphi_1 + \varphi_2}{2}\right)^2}}{\pi} \times FSR \tag{3.3.9}$$

Similarly, the maximum amplitude variation in phase with m_{11} due to input polarization changes is obtained by replacing the η_{1j} in eq. 3.3.7 by their values from eq. 3.2.7 to 3.2.9 (the amplitudes of the sine terms at the 1st order). Therefore:

$$
\begin{cases}
\Delta\eta_{max} = \pm\sqrt{\eta_{12}^2 + \eta_{13}^2 + \eta_{14}^2} \\
\Delta\eta_{max} = \pm\sqrt{\left(\dfrac{\eta_1 - \eta_2}{4}\right)^2 + \left(\dfrac{2\eta_3 - \eta_1 - \eta_2}{4}\right)^2 + \left(\dfrac{2\eta_4 - \eta_1 - \eta_2}{4}\right)^2}
\end{cases}
\tag{3.3.10}
$$

Therefore:

$$
PDL_{dB} \approx 10\log\left(1 + 2\frac{\sqrt{(\eta_1 - \eta_2)^2 + (2\eta_3 - \eta_1 - \eta_2)^2 + (2\eta_4 - \eta_1 - \eta_2)^2}}{\eta_1 + \eta_2}\right) \tag{3.3.11}
$$

Equations 3.3.9 and 3.3.11 permit to properly evaluate the two different DPSK transmission dependences with polarization that come from (i) true *PDL*, that is true loss due to polarization dependence, and (ii) true *PDF*, that is true variation of the interferometer phase due to polarization dependence.

4. CONCLUSION

Until now, the most common technique consisted in computing PDL data by using Müller analysis. PDF was then obtained basically by comparing wavelength at a given signal amplitude for orthogonal polarizations. This technique works well when PDF is of the order of several % of FSR, however, it becomes significantly less precise when PDF is less than 1% of FSR since it suffers from coupling between PDL and PDF along with different loss mechanisms. In this paper, we presented a technique that separates phase measurements from amplitude measurements resulting in a more reliable post-processing technique for retreiving PDF.

Results confirm that this measurement technique is more precise on a wider range (actually no foreseen limits on the domain of validity) of PDL and PDF on tested demodulators. Consequently, we believe it should be considered as a standard method to measure these quantities in MZ interferometers.

REFERENCES

[1] Hentschel C., Schmidt S., “Polarization Measurements using the Agilent 8169A Polarization Controller” Product note available at www.agilent .com

[2] D. Derickson, [Fiber Optic Test and Measurement], Prentice Hall, Chap. 6, (1998)

[3] Bronstein, I. N., Semendjajew, K. A. [Taschenbuch der Mathematik], 24th edition, Teubner Verlagsgesellschaft, Leipzig, (1989)